AIP Journal of Applied Physics

Polarization ratio enhancement of a-plane GaN light emitting diodes by asymmetric two-dimensional photonic crystals

Yen Chou, Hsiang-Wei Li, Yu-Feng Yin, Yu-Ting Wang, Yen-Chen Lin, Da-Wei Lin, Yuh-Renn Wu, Hao-Chung Kuo, and Jian Jang Huang

Citation: Journal of Applied Physics **115**, 193107 (2014); doi: 10.1063/1.4876655
View online: http://dx.doi.org/10.1063/1.4876655
View Table of Contents: http://scitation.aip.org/content/aip/journal/jap/115/19?ver=pdfcov
Published by the AIP Publishing

JOURNAL OF APPLIED PHYSICS 115, 193107 (2014)

Polarization ratio enhancement of a-plane GaN light emitting diodes by asymmetric two-dimensional photonic crystals

Yen Chou,[1] Hsiang-Wei Li,[1] Yu-Feng Yin,[1] Yu-Ting Wang,[1] Yen-Chen Lin,[1] Da-Wei Lin,[2] Yuh-Renn Wu,[1] Hao-Chung Kuo,[2] and Jian Jang Huang[1,a)]

[1]*Graduate Institute of Photonics and Optoelectronics, National Taiwan University, Taipei, Taiwan*
[2]*Department of Photonics and Electro-Optical Engineering, National Chiao-Tung University, Hsinchu, Taiwan*

(Received 21 January 2014; accepted 2 May 2014; published online 20 May 2014)

Fabricating photonic crystals (PhCs) on GaN based non-polar light emitting diodes (LEDs) is an effective way to increase light extraction and meanwhile to preserve or improve polarization ratio. In this work, a-plane GaN LEDs with two-dimensional PhCs were demonstrated. With the E // m polarized modes (which mean the optical polarization with the electric field parallel to m-axis) as the target of diffraction, we matched E//m modes to the photonic bands and aligned E//c modes to fall within the photonic band gap. The results show stronger E//m but weaker E//c mode diffractions on both c- and m-axes. At the vertical direction, the polarization ratio is enhanced from 45.8% for the planar device to 52.3% for the LEDs with PhCs. © *2014 AIP Publishing LLC*.
[http://dx.doi.org/10.1063/1.4876655]

I. INTRODUCTION

With the rapid penetration of light emitting diodes (LEDs) to applications, such as general lighting and backlights of flat-panel displays, there are strong demands to improve bottlenecks that limit LED efficiency. Among them, quantum confined stark effect (QCSE) decreases luminance efficiency and degrades the chromaticity of lighting as colors are shifted with injection currents.[1,2] Non-polar or semi-polar GaN LEDs are developed to suppress QCSE and the corresponding piezoelectric field in the quantum wells (QWs).[3,4] Such devices also exhibit an interesting phenomenon that finds its application in display industry. Generally, common light sources are non-polarized, since the electric field the light has no preferred orientation. However, linearly polarized emissions are obtained in the m-plane or a-plane GaN LEDs, where the asymmetric in-plane biaxial stress on the QWs orients light emitting dipoles preferentially along either the in-plane a- or m-axis, respectively.[5] Polarized light sources can benefit liquid crystal displays which are operated through the spatial modulation of polarized light.[6] Therefore, to achieve linear polarized light, several approaches involving the redesign of epi-layers or device structures have been applied.[7] Epitaxy on non-polar sapphire or free-standing GaN substrates was proposed.[8,9] However, the polarized light was degraded with the adoption of roughened surface to improve light extraction because the polarized photons are randomly scattered. The diffraction of light by optical gratings or photonic crystals (PhCs) offers one possible solution to preserve the polarization and to enhance light-extraction efficiency. A one dimensional (1D) PhC array embedded in the epi-structure has been demonstrated.[10] The PhCs on m-plane LEDs are striping along a-axis. Thus, the intensity of the primary polarized light is enhanced along a-axis direction (E//a). Despite excellent results of the embedded 1D PhCs, there are only a few reports using two dimensional (2D) PhCs[11] on non-polar or semi-polar LEDs with focus, however, not on the performance of polarization ratios.

In this work, 2D PhCs were fabricated on p-type GaN surface of the a-plane LED. We match the E//m (primary polarization of a-plane LED) modes to the photonic band edge (near the band-gap) to increase light extraction. On the other hand, the PhC period along the c-axis is designed to be within the band gap, leading to a weak diffraction of E//c modes. With such a design, we achieve stronger diffraction of E//m modes and weaker one of E//c on both c-axis and m-axis.

II. EXPERIMENT

The a-plane GaN LED epilayers were grown by MOCVD (Metal Organic Chemical Vapor Deposition) on the r-plane sapphire substrate. The LED consists of an AlN nucleation layer, a 2.5 μm-thick Si-doped n-type GaN, 10 pairs of InGaN (3 nm)/GaN (12 nm) MQWs, and a 200 nm-thick Mg-doped p-type GaN layer. Peak emission wavelength is at around 520 nm. The device fabrication started from electron-beam lithography to define PhCs. The period is 320 nm along c-axis and 260 nm along m-axis, constituting a rectangular PhC array with the depth of 70 nm (see the scanning electron microscopic (SEM) picture in Fig. 1(a)). With E//m modes as the target of diffraction, the periods on both axes are designed so that E//m peak frequencies fall on the PhC band edge (at the normalized frequency 0.6 on c-axis and 0.5 on m-axis), which they experience large group index variation, and thus E//m modes can be intensively diffracted.[12] On the other hand, the larger photon energy E//c modes are designed to be less diffracted by the PhCs. The subsequent process steps involve mesa definition, n- and p-type metallization, and alloy. The device structure is shown in Fig. 1(b).

To investigate the diffraction characteristics of E//m and E//c modes, we analyzed the emission contours converted

a)Electronic mail: jjhuang@ntu.edu.tw

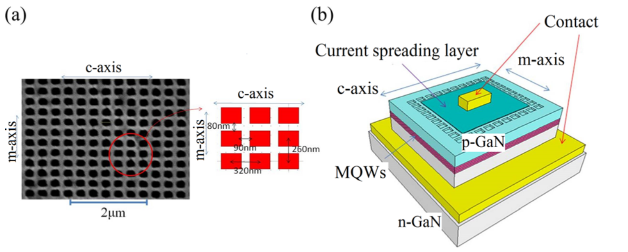

FIG. 1. (a) The SEM image of the PhCs on a-plane GaN LED. (b) Schematic diagram of the PhC LED. The m-axis is in the horizontal direction while the c-axis is in lateral direction. The PhC period and spacing are 320 and 90 nm, and 260 nm and 80 nm, for c- and m-axis, respectively. (b) Schematic diagram of the device structure. The current spreading layer is to ensure more uniform distribution of the injection currents so that the generated photos can be uniformly interact with top PhC structure.

from the polarized angular-resolved spectral measurement on the a-c and a-m planes.[12,13] In the measurement, a polarizer was placed between the device and detector so that the radiation profiles of E//m and E//c polarized light were collected. The angular spectra were then converted to the photonic band structure (the method can be referred from Ref. 10).

III. RESULTS AND DISCUSSIONS

The measured photonic bands are shown in Fig. 2. Other than the obvious Fabry-Perot resonance between GaN/air and GaN/sapphire interfaces, diffractions modes are observed as illustrated by the dashed lines with positive and negative group indexes in the contours. The diffractions are mainly due to photons interacted with PhCs along the c-axis and m-axis. The guiding modes at these locations are diffracted out to the air because they experience abrupt changes in group indexes,[12] which can be observed from the crossings of diffracted modes (the crossings of lines). The positive and negative slopes of the photonic bands in Figs. 2(a) and 2(b) also imply positive and negative group indexes, respectively. On the other hand, the corresponding E//c normalized frequency (a/λ, which a is period of PhC, and λ is the wavelength of light modes, the normalized frequency identifies the possible emission wavelength or frequency from the photonic bands) is slightly off the photonic band edge along both c- and m-axes. Therefore, E//c modes experience relatively weaker group index variations, as indicated in Figs. 2(c) and 2(d) that no obvious mode crossings are presented. Hence, the diffraction of E//m modes is more intensive than that of E//c modes. For this reason, we can enhance the polarization ratio by the asymmetric design of PhCs along c- and m-axes.

The light output power of PhC and planar LEDs at different current injections is shown in Fig. 3. At 20 mA, light output of the PhC LED increases by 44.87% as compared to that of the planar device, which the enhancement is mainly due to the two-dimensional PhC structure. Despite the enhancement of total light output power, we see an asymmetric light output increase between E//m and E//c modes, which will be further discussed latter.

The variation of group indexes in the emission contours determines the radiation patterns. As illustrated in Fig. 4(a), the positive refractive index basically contributes a forward emission, while the backward diffraction is attributed to the negative index. For the emission contours in Figs. 2(a) and 2(b), the optical modes experience abrupt variation of group indexes during the propagation and light extraction at the band crossings,[12] leading to the congregation of photons at smaller angle ranging from 3° to 20°. In Fig. 4(b), for the E//m mode emission profile, photons congregate at a smaller angle with respect to the in-plane k-vectors ($k_{||}$) around $3–5 \times 10^6\,m^{-1}$ (a-c scan) and $0.5–3 \times 10^6\,m^{-1}$ (a-m scan).

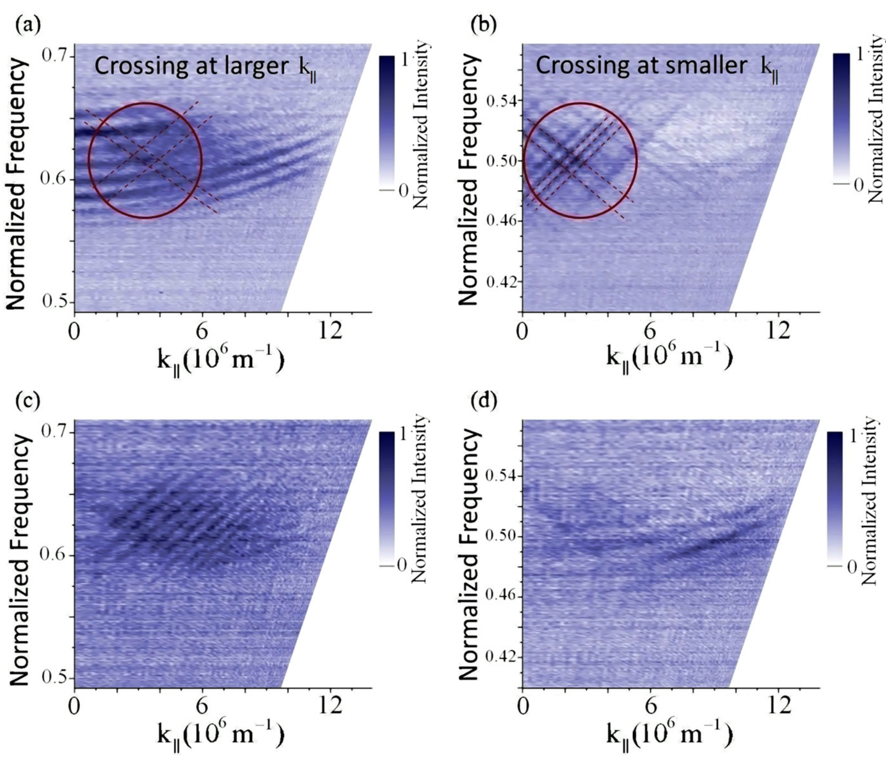

FIG. 2. Photonic bands by mapping the emission contours to the normalized frequency and in-plane wavevector. (a) represents E//m mode photonic bands in a-c plane scan; (b) is E//m modes in a-m plane scan; (c) is E//c modes in a-c plane scan; (d) is E//c modes in a-m plane scan.

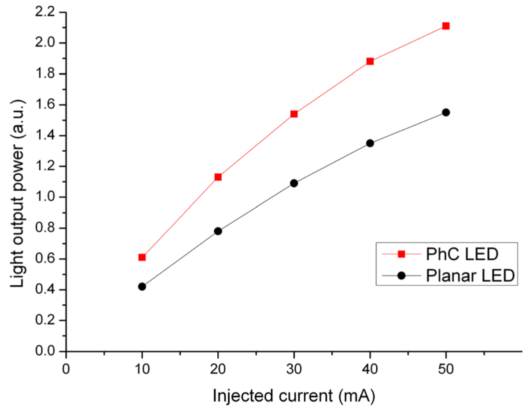

FIG. 3. The light output power of PhC LED and planar LED at different injected current.

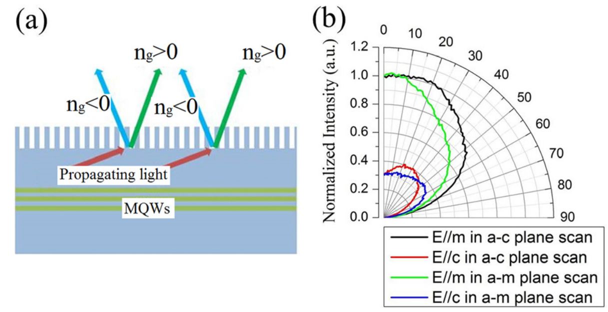

FIG. 4. (a) Illustration of light diffractions as the laterally guide modes experience positive or negative group index (b) Radiation profiles of E//m and E//c modes under a-c and a-m scans at an injection current of 20 mA.

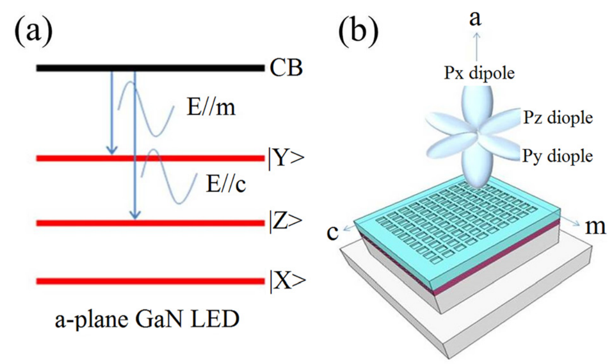

FIG. 5. (a) Illustration of a-plane QW valence band splitting and the corresponding emission from |Y⟩ and |Z⟩ states (band structure is not according to realistic scale). (b) The polarization orientation of the radiation from the sub-band. The radiation from |X⟩ states is usually neglected.

On the other hand, E//c modes experience only either positive or negative group index. Therefore, E//c modes tend to spread out to a wider radiation profile without gathering the extracted light at certain angles.

The maximum intensities are located at 16° (a-c scan) and 3° (a-m scan) for E//m modes at the injection current of 20 mA. As for the E//c modes emissions, the peak intensities occur at 31° (a-c scan) and 50° (a-m scan). The following equation can trace the in-plane k-vector, $k_{\|}$

$$k_{\|} = \frac{2\pi}{\lambda} \sin\theta, \quad (1)$$

which λ is the wavelength and θ is the escape angle of light from the surface normal. We found that with known angles of maximum intensity (16° and 3°), $k_{\|}$ at the strongest diffractions can be determined to be $3.3 \times 10^6\,\mathrm{m}^{-1}$ for a-c scan and $5.6 \times 10^5\,\mathrm{m}^{-1}$ for a-m scan. The results are close to those obtained from the photonic band crossings in Figs. 2(a) and 2(b). They also imply that side lobes in the radiation profiles occur when the photons accumulate at the crossings of photonic bands.

To further investigate the emissions on c-axis and m-axis with the designated periods of PhC, we analyzed the emission contours in the a-c and a-m plane scans. The emission characteristics of E//m modes on a-m plane show differences to its counterpart along a-c plane. The optical intensity congregates to the smaller $k_{\|}$, which can be explained based on the phase matching equation

$$k'_{\|} = k_{g,\|} + pG. \quad (2)$$

In (2), the diffraction vector G is $2\pi/a$, where a is PhC period, and p is an integer. $k_{g,\|}$ is the in-plane k-vector of a guided mode. $k'_{\|}$ is the out-coupled mode of the in-plane k-vector. With a smaller PhC period, the diffraction vector G becomes larger and thus $k'_{\|}$ for phase matching tends to adjust itself toward a smaller value, leading the radiated intensity at a smaller angle. The discussion can be verified from Fig. 4(b). With a smaller period along m-axis, the radiated energy of E//m modes along a-m plane gathers at a smaller angle.

One of the critical properties that differentiate non-polar LED structure from the c-plane one is the mitigation of QCSE. With the incorporation of PhCs, the polarization of photons is further re-distributed. Thus, the polarization ratio of our device is larger than that of the planar devices. Table I lists the polarization ratios along a-c and a-m scans of both the planar and PhC devices. Polarization ratio, ρ, is defined as

$$\rho = \frac{I_{E\|m} - I_{E\|c}}{I_{E\|m} + I_{E\|c}}, \quad (3)$$

where $I_{E\|m}$ is the intensity of E//m modes, and $I_{E\|c}$ is the intensity of E//c modes. With E//m modes as the main

TABLE I. Polarization ratios of the PhC and planar LEDs along the a-m and a-c scans.

Scan orientations	PhC LED (at 0°)	Planar LED (at 0°)	PhC LED (integrated of all the angles) %	Planar LED (integrated of all the angles) %	At the angle of maximum E//m intensity
a-c scan	52.3%	45.8%	45.3	41.9	46.4% (at 16°)
a-m scan			36.9	34.2	50% (at 3°)

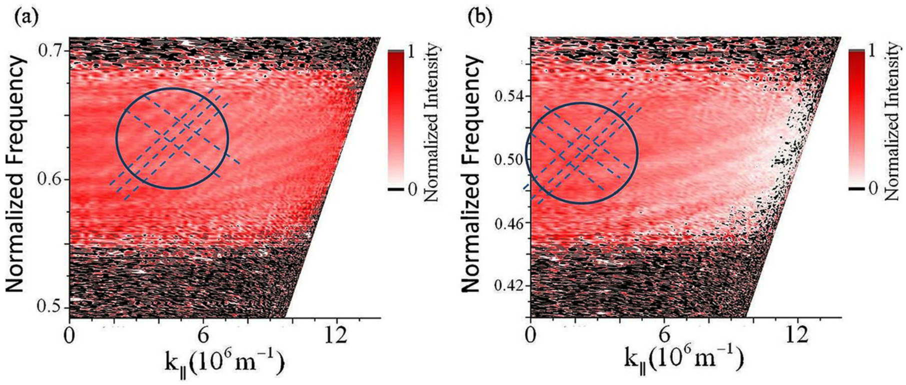

FIG. 6. Polarization ratio contours under the a-c plane (a) and a-m plane (b) at various normalized frequencies and wavevectors.

diffraction target, PhCs not only diffract photons along the c-axis but also the m-axis, which means that polarization ratios of both a-c and a-m planes are enhanced. The increase of polarization ratio applies not only to vertical emission but also to the integrated intensities of the radiation profiles along a-c and a-m scans. In Table I, the polarization ratios at the angles of maximum E//m mode intensities along a-c and a-m plane are also recorded (in this case, 16° on a-c plane, and 3° on a-m plane).

In Table I, however, the polarization ratios of the integrated intensity in the a-m plane scan are lower than those in the a-c scan. It is mainly attributed to the fact that E//m mode propagation along m-axis is off-axis.[10] That is, for the emission from the $|Y>$ state sub-band (see the axis definition in Fig. 5), the propagation direction of E//m modes is mainly determined by the P_y dipole, and the most of the light emission propagates along the a-c plane. $k_{\parallel}$ of E//m modes is mainly aligned on c-axis (that is, "on-axis"). In contrast, the E//m energy off c-axis accounts for only a small portion of the overall E//m emission. On the contrary, for E//c modes, their on-axis is along a-m plane. Thus, while a large part of E//c mode and a smaller part of E//m energy propagate along the a-m plane, the absolute E//m mode intensity is still larger than E//c one. The integrated polarization ratio of all the angles decreases in the a-m scan. The radiation profile in Fig. 4(b) agrees with our explanations by showing the intensity of the E//m radiation on the a-m plane is much less than that on a-c scan.

We further correlate the polarization ratios to the photonic band contours. Demonstrated in Fig. 6, the polarization ratio contours follow a similar trend to the light emission diagrams in Figs. 2(a) and 2(b). The crossings of the emission band profiles in Figs. 2(a) and 2(b) matches these of the polarization ratio contours in Fig. 6 at nearly the same normalized frequency and in-plane wavevector. The similarity of the contours in both emission (photonic bands) and polarization ratio suggests that the latter is dominated by the E//m mode emission, which is also the dominant radiation among the split bands (as shown in Fig. 5). In addition, E//m modes, which are enhanced by the PhCs, are more intensively diffracted than the E//c modes, leading to the increase of the polarization ratio along a-c and a-m planes. The above results verify the polarization ratio enhancement from the diffraction of E//m modes by PhCs.

IV. CONCLUSION

In this research, we applied two-dimensional PhCs on both c-axis and m-axis of the a-plane LED to diffract mainly the E//m guiding modes. The photonic bands based on the emission contours were analyzed. The intense diffraction of E//m modes leads to large group index variations. The photons accumulated at the locations of small k vectors where positive and negative slopes of photonic bands encounter. On the other hand, the diffraction of E//c modes is weak as there are no obvious crossings of positive and negative slopes. Thus, E//c modes tend to spread out. The contours of polarization ratios show similar behaviors to the emission profiles. The polarization ratios are 45.3% (a-c scan) and 36.9% (a-m scan) of the PhC LED device, compared with 41.9% (a-c scan) and 34.2% (a-m scan) for the planar a-plane sample. The above results indicate that PhC can redistribute the photon energy of E//m and E//c modes. The design of PhC structure has the direct influence on the amount of photon accumulations in the diffracted modes. It also selectively interacts with specific modes (e.g., E//m modes) so that more photons are extracted to the air. The polarization ratio is enhanced with the above consideration.

ACKNOWLEDGMENTS

We thank the National Science Council in Taiwan for the financial support of this study under the Grant Nos. NSC 100-2628-E-002-030-MY3 and 102-2218-E-002-002-.

[1]S. Chichibu, T. Azuhata, T. Sota, and S. Nakamura, Appl. Phys. Lett. **69**, 4188 (1996).
[2]P. Waltereit, O. Brandt, A. Trampert, H. T. Grahn, J. Menniger, M. Ramsteiner, M. Reiche, and K. H. Ploog, Nature **406**(6798), 865 (2000).
[3]C. H. Chiu, S. Y. Kuo, M. H. Lo, C. C. Ke, T. C. Wang, Y. T. Lee, H. C. Kuo, T. C. Lu, and S. C. Wang, J. Appl. Phys. **105**, 063105 (2009).
[4]A. Bhattacharyya, I. Friel, S. Iyer, T. C. Chen, W. Li, J. Cabalu, Y. Fedyunin, K. F. Ludwig, T. D. Moustakas, and H. P. Maruska, J. Cryst. Growth **251**(1), 487 (2003).
[5]H. Masui, H. Yamada, K. Iso, J. S. Speck, S. Nakamura, and S. P. DenBaars, J. Soc. Inf. Disp. **16**(4), 571 (2008).
[6]H. J. Cornelissen, H. J. B. Jagt, D. J. Broer, and C. W. M. Bastiaansen, Proc. SPIE **7058**, 70580X1 (2008).
[7]M. Koike, N. Shibata, H. Kato, and Y. Takahashi, IEEE J. Sel. Top. Quantum Electron. **8**(2), 271 (2002).

[8]A. Chakraborty, B. A. Haskell, S. Keller, J. S. Speck, S. P. Denbaars, S. Nakamura, and U. K. Mishra, Jpn. J. Appl. Phys., Part 2 **44**, L173 (2005).
[9]M. C. Schmidt, K. C. Kim, H. Sato, N. Fellows, H. Masui, S. Nakamura, S. P. DenBaars, and J. S. Speck, Jpn. J. Appl. Phys., Part 2 **46**, L126 (2007).
[10]E. Matioli, S. Brinkley, K. M. Kelchner, Y. L. Hu, S. Nakamura, S. P. DenBaars, J. S. Speck, and C. Weisbuch, Light: Sci. Appl. **1**(8), e22 (2012).
[11]T. T. Wu, S. Y. Lo, H. M. Huang, C. W. Tsao, T. C. Lu, and S. C. Wang, Appl. Phys. Lett. **102**(19), 191116 (2013).
[12]Y. F. Yin, Y. C. Lin, T. H. Tsai, Y. C. Shen, and J. J. Huang, Opt. Lett. **38**(2), 184 (2013).
[13]Y. W. Cheng, K. M. Pan, C. Y. Wang, H. H. Chen, M. Y. Ke, C. P. Chen, M. Y. Hsieh, H. M. Wu, L. H. Peng, and J. J. Huang, Nanotechnology **20**(3), 035202 (2009).